

Supplementary Information

Microfluidic capillary transit velocity as a functional measure for sickle cell disease and in vitro-derived red blood cells

Solomon Oshabaheebwa¹, Utku Goreke², Yuxuan Du³, Christopher L. Wirth⁴, Zoe Sekyonda¹, Bryan Benson⁵, Payam Fadaei³, Yusang B. Ley¹, Nathan M. Perez², Petros Giannikopoulos², David N Nguyen^{2,6,7}, Michael A. Suster⁸, Pedram Mohseni^{1,8,*}, Umut A. Gurkan^{1,3,*}

Affiliations:

¹Department of Biomedical Engineering, Case Western Reserve University, Cleveland, OH, USA.

²Innovative Genomics Institute, University of California, Berkeley, CA, USA

³Department of Mechanical and Aerospace Engineering, Case Western Reserve University, Cleveland, OH, USA

⁴Department of Chemical and Biomolecular Engineering, Case Western Reserve University, Cleveland, OH, USA

⁵Cleveland Clinic; Cleveland, OH, USA.

⁶Department of Medicine, University of California, San Francisco, CA, USA.

⁷Department of Molecular and Cell Biology, University of California, Berkeley, CA, USA

⁸Department of Electrical, Computer, and Systems Engineering, Case Western Reserve University, Cleveland, OH, USA.

***Co-Corresponding authors:**

Pedram Mohseni, PhD

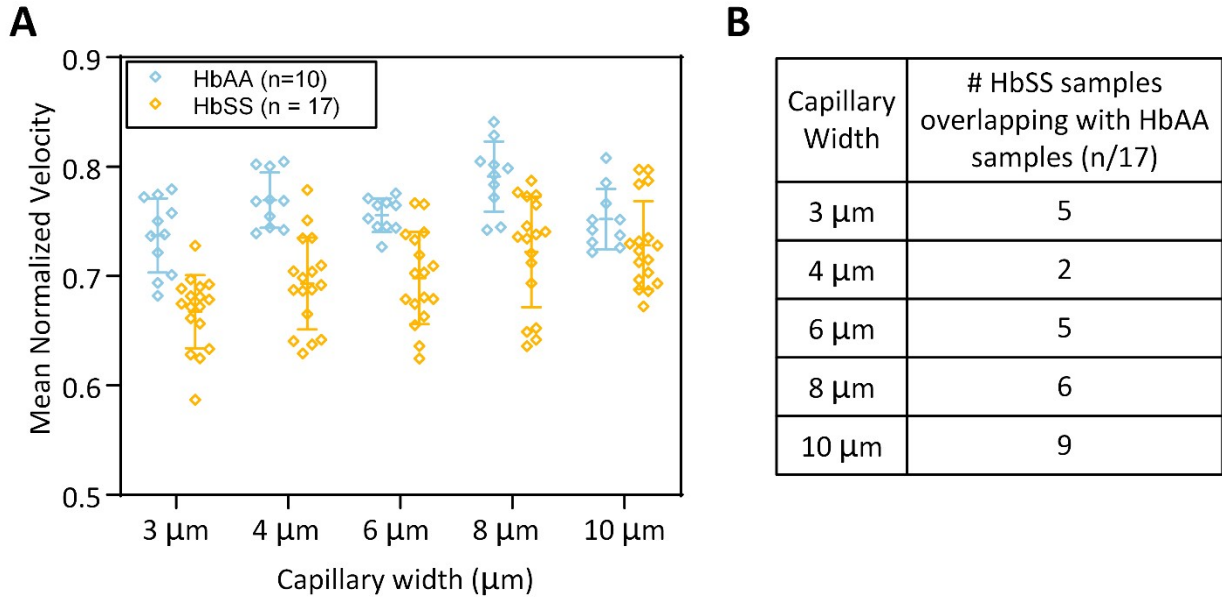
Department of Electrical, Computer, and Systems Engineering, Case Western Reserve University, Cleveland, OH, 44106, USA. Email address: pxm89@case.edu, Tel: +1 (216) 368 5263

Umut A. Gurkan, PhD

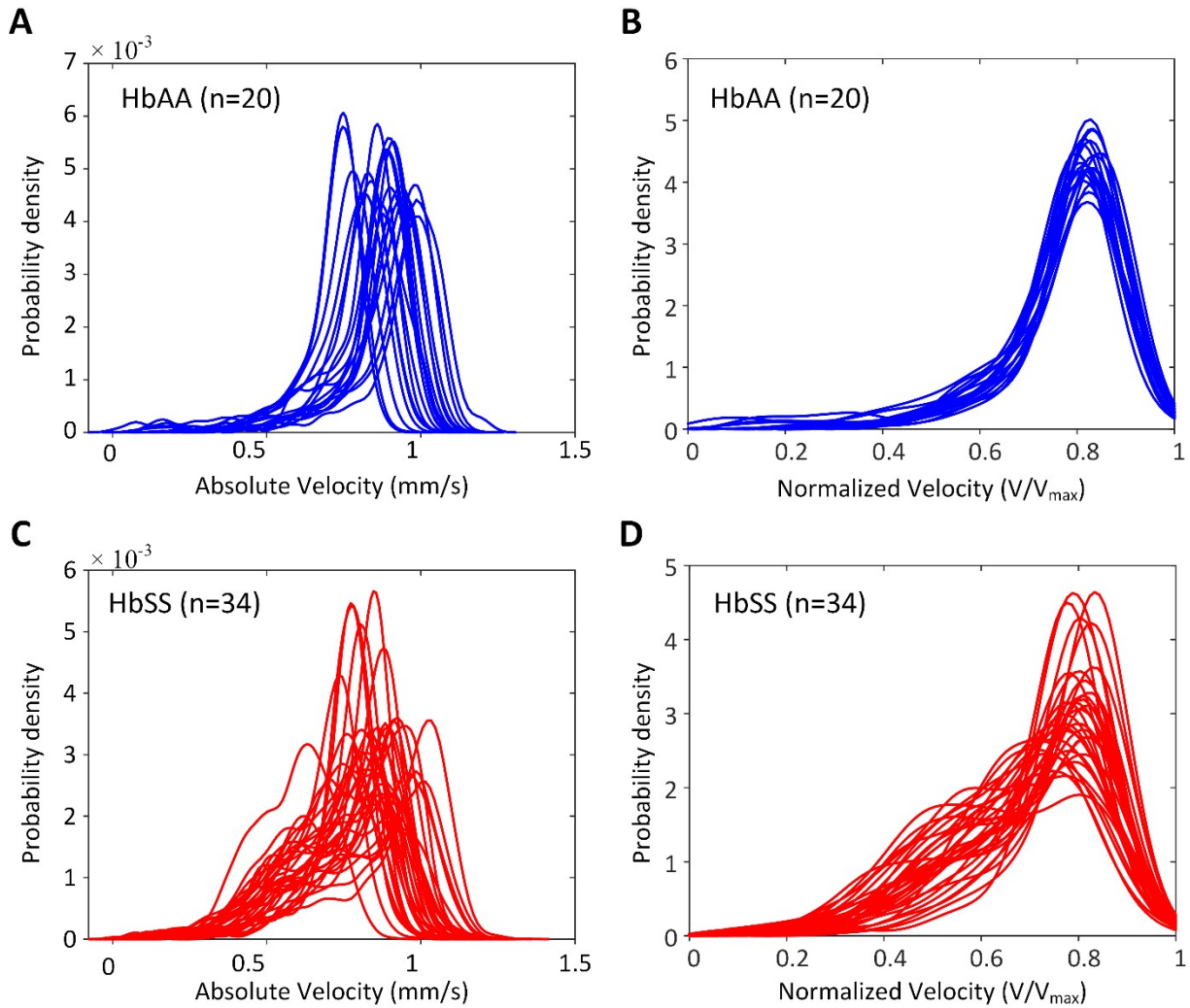
Department of Mechanical & Aerospace Engineering, Case Western Reserve University, Cleveland, OH, 44106, USA. Email address: umut@case.edu, Tel: +1 (216) 368-6447

Keywords:

Microcirculation, Velocimetry, Rheology, Microfluidics, In vitro differentiated RBCs, GBT021601, RBC mechanics, Capillary transit time heterogeneity, Gene therapy, RBC Morphology

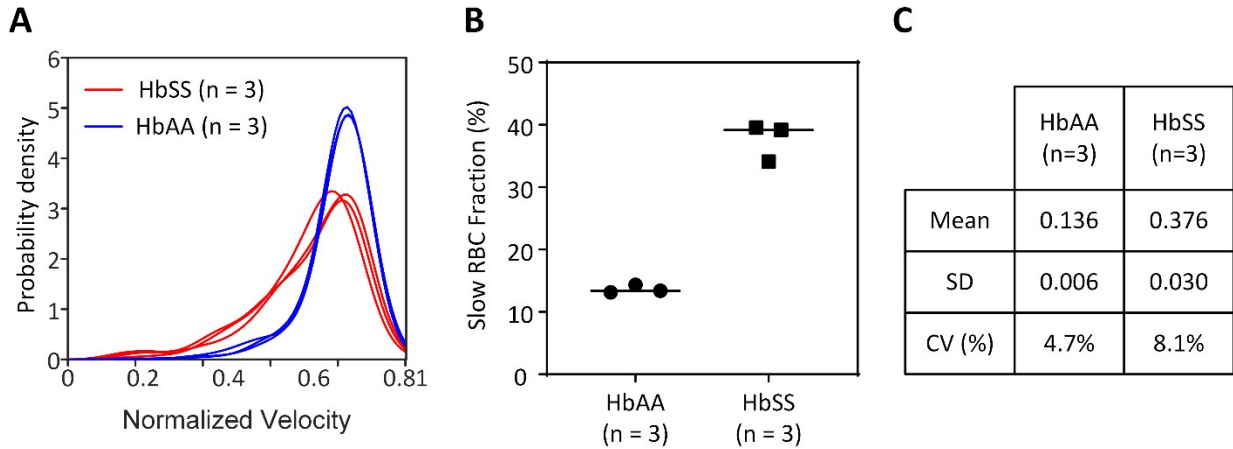


Supplementary Figure S1: Determination of the optimal capillary array for RBC velocity assessment. (A) Mean normalized velocity of RBCs from 10 HbAA samples and 17 HbSS samples at five discrete capillary sizes. (B) The table shows the number of HbSS samples (out of 17 total) overlapping with HbAA samples (n= 10). The 4 μm -wide capillary array was used in subsequent experiments since it showed the best separation with only 2/17 HbSS samples overlapping with HbAA samples.

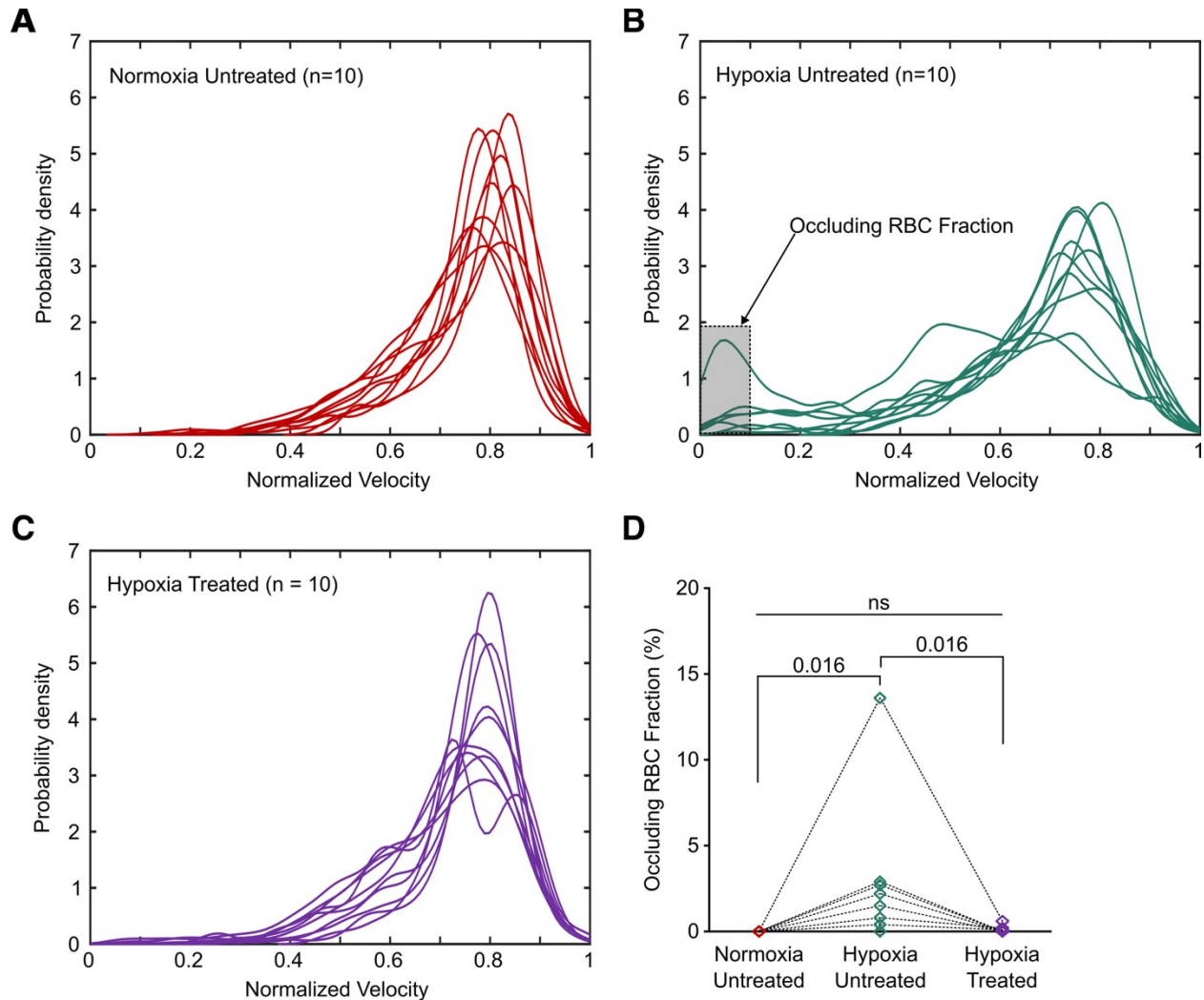


Supplementary Figure S2: Effect of normalization on velocity measurement.

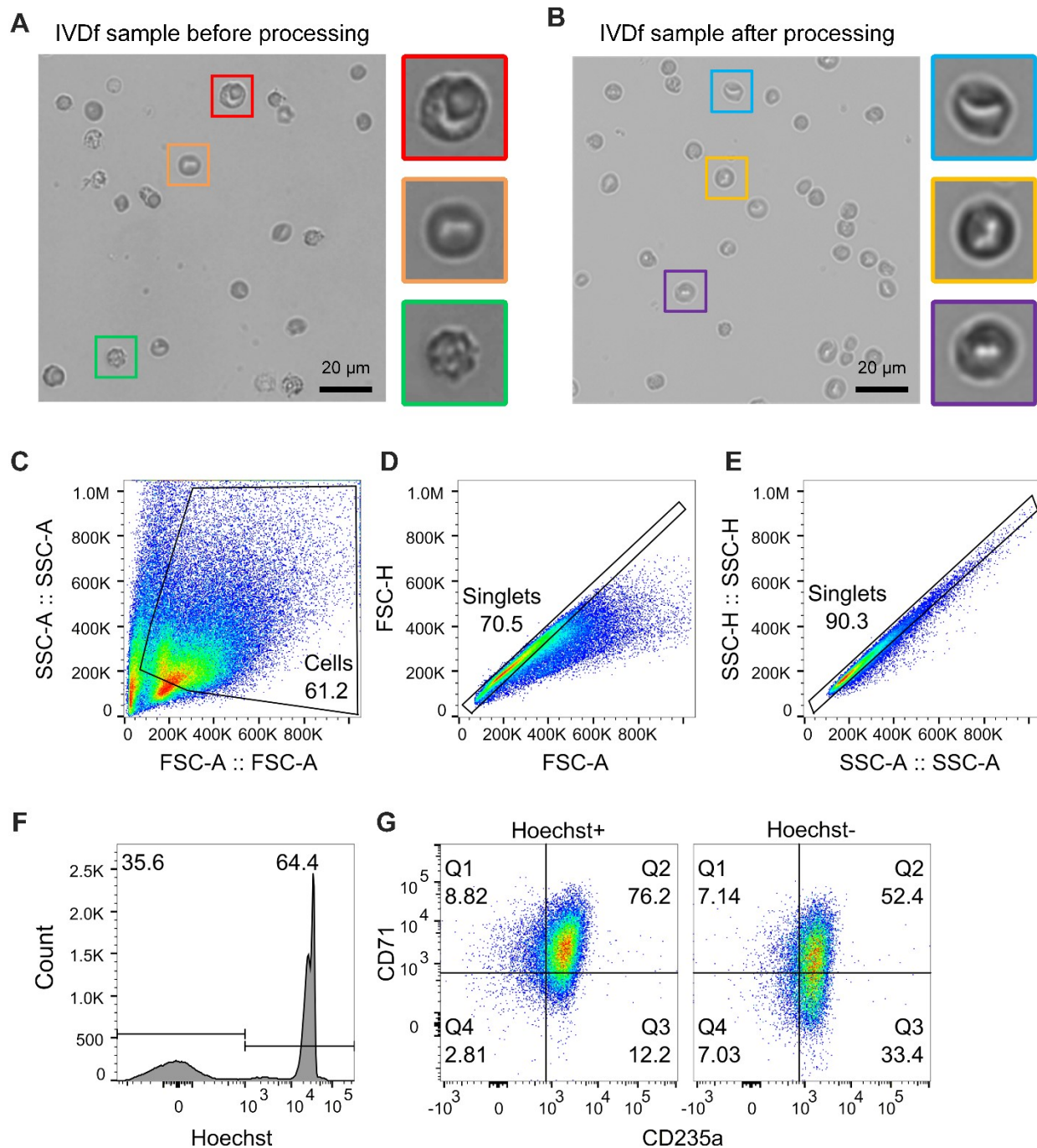
Normalized Velocity was obtained by dividing all RBC velocities in each experiment by the maximum RBC velocity recorded in that experiment. Panel A shows the absolute velocities of 20 HbAA samples, which exhibit wide variation in their velocity profiles. Panel B shows the same data after normalization, where the profiles follow a similar trend with the variation significantly reduced. Panels C to D show a similar correction in 34 HbSS samples. The absolute velocity was 0.82 ± 0.06 mm/s in HbAA samples versus 0.75 ± 0.06 mm/s in HbSS samples.



Supplementary Figure S3: Reproducibility of the assay. Reproducibility was assessed by running one HbSS sample and one HbAA sample, each on three different devices (triplicate experiments). (A) RBC Velocity distribution profiles for the triplicate HbSS and HbAA samples. (B) Each data point represents the slow RBC fraction obtained from the profiles in panel A. (C) The table shows the mean, standard deviation (SD), and coefficient of variance (CV) of the slow RBC fraction for each sample type. These results demonstrate that the assay is reproducible with a CV of 4.7% for HbAA samples and 8.1% for HbSS samples.



Supplementary Fig. S4: Effect of hypoxia on RBC velocity. Velocity distribution profiles showing ten individual HbSS samples under (A) normoxia, (B) hypoxia untreated, and (C) hypoxia with GBT021601 treatment. (D) The occluding RBC fraction, defined as the fraction of RBCs with a normalized velocity less than 0.1, was 0% under normoxia, $2.4\% \pm 4.0\%$ under hypoxia untreated, and $0.1\% \pm 0.2\%$ under hypoxia with GBT021601 treatment. The patient with a uniquely high number of occluding RBCs under hypoxia untreated was on supportive therapy and had not been recently transfused.



Supplementary Fig. S5: Characterization of *in vitro*-derived cells via microscopy and flow cytometry. (A) Before processing, the sample contained a wide variety of cell shapes including nucleated cells (red insert), biconcave RBCs (orange insert), and

granular cells (green insert). **(B)** The processed sample comprised predominantly biconcave RBCs, as shown in the inserts. **(C-G)** Flow Cytometry analysis of CD235a / CD71 expression in the invitro-derived RBCs, shown for both nucleated (Hoechst+) and enucleated (Hoechst-) cells. Panels C – E show the gating strategy, starting with selection of Cells based on size (FSC-A) and granularity (SSC-A), followed by Singlets selection using FSC-A vs FSC-H and SSC-A vs SSC-H. Panel F shows the proportion of Hoechst+ (64.4%), and Hoechst- (35.6%), and panel G shows CD235a / CD71 expression in the respective populations. Gating thresholds were determined using T cells and verified with unstained cells as controls.